# ROBUST CONTROL IN ROTOR MACHINES USING LINEAR MATRIX INEQUALITIES

**Edson Hideki Koroishi, koroishi@mecanica.ufu.br**[1]
**Aldemir Aparecido Cavalini Júnior, aacjunior@mecanica.ufu.br**[1]
**Valder Steffen, Jr, vsteffen@mecanica.ufu.br**[1]

[1] Federal University of Uberlândia (UFU) - School of Mechanical Engineering - Campus Santa Mônica, Av. João Naves de Ávila 2121, Bloco 1M, Uberlândia, MG, Brazil, ZIP CODE 38400-902, http://www.mecanica.ufu.br/

*Abstract. Some methods of Active Vibration Control (AVC) are model-based; in these cases the parameter variations have an important issue in the performance of the system. As it is not possible to know in advance the precise values of these parameters of the mechanical system, a possible alternative is to design robust controllers that take into account the uncertainties involved. In this sense, this paper presents an active vibration control technique that is dedicated to rotating machinery by incorporating Electromagnetic Actuators (EMA) so that uncertainties are taken into account with respect to the parameters of the system. The EMA's gains are determined by using Linear Matrix Inequalities (LMIs). The LMIs are a powerful tool in the cases the system presents uncertainties in its parameters. The Kalman Estimator was used to access the modal states of the system. The model of the rotating machinery is obtained by using the Finite Element Method (FEM). Simulation results illustrate the potential use of the methodology conveyed in engineering applications.*

*Keywords: Robust Control, Electromagnetic Actuator, Kalman Estimator, LMIs*

## 1. INTRODUCTION

A number of types of actuators are available for control purposes, such as Piezoelectric Stack Actuators, Active Magnetic Bearings (AMB), and Electromagnetic Actuators (EMA). The Piezoelectric Actuators demonstrated to be very effective in rotor vibration control (Palazzolo et al, 1993). More recently (Simões et al, 2007) presented an active modal control strategy for flexible rotors by using two orthogonal PZT stack actuators installed at one of the supports of the machine, i.e., the PZT actuators were attached directly to the ball bearing, which allows the insertion of stiffness to the system. The AMB have been successfully applied in industrial turbomachines (Schweitzer et al, 2009). The AMB provide control effort through the application of lateral forces without mechanical contact between the rotor and the stator. However, they have some disadvantages, technical complexity and continuous power consumption (Horst et al, 2004), which is due to rotor support requirements.

The EMA uses the same physical principle of the AMB, but only in terms of the lateral force without contact, since the EMA is not used to support the rotor. The use of EMA results in a hybrid bearing. The active control using EMA was achieved successfully both numerically and experimentally in light structures (Der Hagopian et al, 2010). The advantage of EMA is due to the simple electromechanical structure associated with the control action, without mechanical contact.

In the context of countless demands of mechanical systems with optimal performance, this work proposes to design a robust controller for a rotor system by using electromagnetic actuators (EMAs). The EMAs were arranged around the rotor as shown in Fig. (1). Together with the ball bearing, the resulting architecture forms a so-called hybrid bearing.
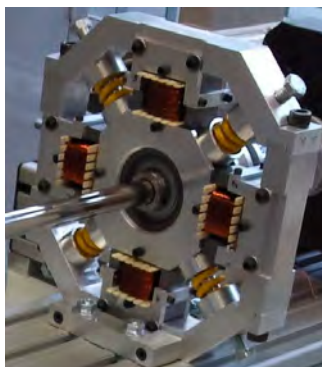


Figure 1. Hybrid bearing.

The linear quadratic regulator (LQR) approach, solved by linear matrix inequalities (LMI), allows for the calculation of the gain matrix of the feedback controller.

LMI is a useful tool for constrained problems in which the parameters vary according to a given range of values. Once formulated in terms of LMIs the problem can be solved efficiently by convex optimization algorithms (Boyd et al, 1994). The advantage of using LMIs for determining the controller gain matrix is the possibility of assuming that the parameters of the model involve uncertainties. Then, a robust vibration control system can be designed.

## 2. ROTOR FINITE ELEMENT MODEL

The dynamic response of the considered mechanical system can be modeled by using principles of variational mechanics, namely the Hamilton`s principle. For this aim, the strain energy of the shaft and the kinetic energies of the shaft and discs system are calculated. An extension of Hamilton`s principle make possible to include the effect of energy dissipation. The parameters of the bearings are included in the model by using the principle of the virtual work. For computation purposes, the FEM is used to discretize the structure so that the energies calculated are concentrated at the nodal points. Shape functions are used to connect the nodal points. To obtain the stiffness of the shaft the Timoshenko`s beam theory was used and the cross sectional area was updated. The model obtained as described above is represented mathematically by a set of differential equations (Lalanne et al, 1997) as given by Eq. (1).

$$[M]\{\ddot{\delta}(t)\} + [C_b + \dot{\phi}C_g]\{\dot{\delta}(t)\} + [K + \phi K_g]\{\delta(t)\} = \{F(t)\} + \{F_{EMA}(t)\} \tag{1}$$

where $\{\delta(t)\}$ is the vector of generalized displacements; $[M]$, $[K]$, $[C_b]$, $[C_g]$ e $[K_g]$ are the well-known matrices of inertia, stiffness, bearing viscous damping (that may include proportional damping), gyroscopic (with respect to the speed of rotation), and the effect of the variation of the rotation speed; $\dot{\phi}$ is the time-varying angular speed, and $\{F(t)\}$ e $\{F_{EMA}(t)\}$ are the forces due to the unbalance and to the electromagnetic actuator, respectively.

The use of a larger number of degrees of freedom (dof) results in a high computational cost. Normally it is desirable to reduce the size of the model. There are several methods that can be used for this aim [20], however, the pseudo-modal method is used in the present paper to reduce the model size. The reduction is achieved by changing from the physical coordinates $\{\delta(t)\}$ to modal coordinates $\{q(t)\}$ as follows:

$$\{\delta(t)\} = [\Phi]\{q(t)\} \tag{2}$$

where $[\Phi]$ is the modal basis that contains the $m$ first modes of the non-gyroscopic conservative associated system.

By using the transformation given by Eq. (2) in the Eq. (1), and by converting the new set of differential equations to the space-state form results:

$$\begin{aligned}\{\dot{X}(t)\} &= [A]\{X(t)\} + [B_w]\{F(t)\} + [B_u]\{F_{EMA}(t)\} \\ \{y(t)\} &= [C]\{X(t)\}\end{aligned} \tag{3}$$

where

$$\{X(t)\} = \begin{Bmatrix} \{q(t)\} \\ \{\dot{q}(t)\} \end{Bmatrix}$$

$$[A] = \begin{bmatrix} 0 & I \\ -[[\Phi]^T[M][\Phi]]^{-1}[[\Phi]^T[K][\Phi]] & -[[\Phi]^T[M][\Phi]]^{-1}[[\Phi]^T[C][\Phi]] \end{bmatrix}$$

$$[B_w] = \begin{bmatrix} 0 \\ [[\Phi]^T[M][\Phi]]^{-1}[\Phi]^T \end{bmatrix}$$

$$[B_u] = \begin{bmatrix} 0 \\ [[\Phi]^T[M][\Phi]]^{-1}[\Phi]^T \end{bmatrix}$$

$$[C] = [[\Phi]]$$

The number of considered modes is defined according to the controllability and observability of the system represented by Eq. (3). In this work the number of modes considered is four (two for each direction) so that the system is controllable and observable. The rotor´s model was developed based on the rotor test rig presented in Fig. (2).
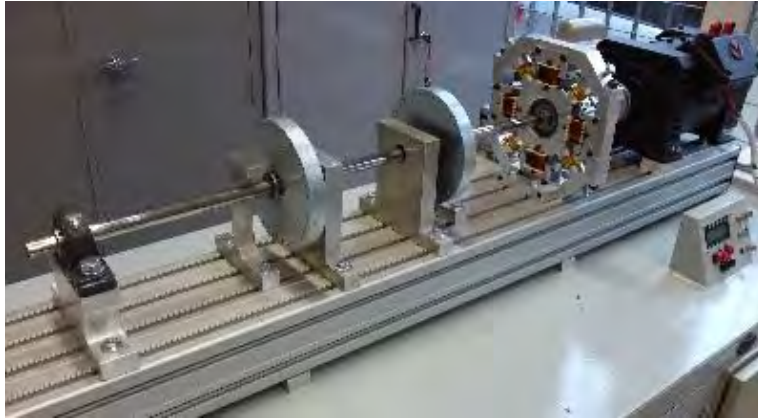


Figure 2. Rotor Test Rig.

Figure 3 presents the FE model in which 32 finite elements are used to represent the dynamic behavior of the rotor. It is composed of a flexible steel shaft with 80 mm length and 17 mm diameter ($E_{steel}$ = 2.1 $X$ $10^{11}$ Pa, $\rho_{steel}$ = 7850 kg/m$^3$, and $\nu_{steel}$ = 0.3), two rigid steel discs located at the nodes #13, and #22, respectively, and two roller bearings ($B_1$ and $B_2$ located at the nodes #4 and #31, respectively). The nominal stiffness and damping parameters of the bearings are summarized in Tab. (1). Damping was added in the rotor by means of a proportional damping ($D_p = \alpha M + \beta K$; $[M]$ and $[K]$ being the mass and stiffness matrices, respectively) with the following nominal coefficients: $\alpha = 10$ and $\beta = 1$ $X$ $10^{-5}$. Displacement sensors are orthogonally mounted (along the horizontal and vertical directions) at the nodes #8 and #25 to collect the shaft vibration. The first twelve vibration modes were used to generate the displacement responses of the rotor model along the orthogonal directions. The Electromagnetic Actuators (EMAs) are located at the node #4, which corresponds to the position of the bearing $B_1$.
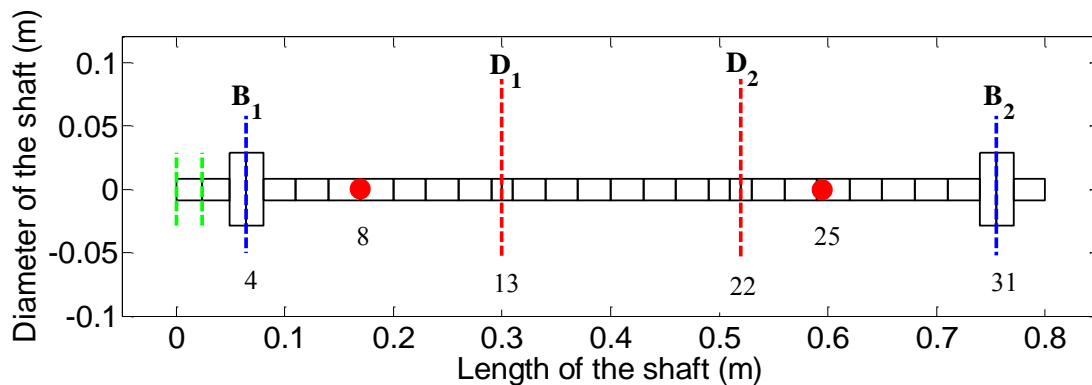


Figure 3. FE model of the considered rotor (- - - - Bearing;
- - - - Disc; - - - - Coupling # node).

The properties of the bearings are presented in Tab. (1).

Table 1. Physical characteristics of the bearings

| Characteristic | Value |
|---|---|
| **Bearings** | |
| $k_{x1}$ (N/m) | 1.00X10$^6$ |
| $k_{z1}$ (N/m) | 1.30X10$^6$ |
| $k_{x2}$ (N/m) | 1.00X10$^8$ |
| $k_{z2}$ (N/m) | 1.00X10$^8$ |
| $c_{x1}$ (N.s/m) | 60 |
| $c_{z1}$ (N.s/m) | 60 |
| $c_{x2}$ (N.s/m) | 100 |
| $c_{z2}$ (N.s/m) | 100 |

Koroishi, E. H., Cavalini Jr, A. A., Steffen Jr, V.
Robust Control in Rotor Machines using Linear Matrix Inequalities

## 3. LINEAR MATRIX INEQUALITIES

The history of LMIs in the analysis of dynamical systems goes back more than 100 years. In 1890, Aleksandr Mikhailovich Lyapunov presented his work, introducing the Lyapunov Theory (Boyd et al, 1994), showing that the differential equation:

$$\{\dot{x}(t)\} = [A]\{x(t)\} \tag{4}$$

is stable (all the trajectories converge to zero) if and only if there is a positive-definite matrix P such that:

$$[A]^T[P] + [P][A] > 0 \tag{5}$$

The inequality given by Eq. (5) is known as the Lyapunov inequality.

Currently, LMIs have been the object of study to many important researchers around of the world focusing a number of different problems: control of continuous and discrete systems in the time domain, optimal control and robust control (Van Antwerp et al, 2000; Silva et al, 2004) model reductions (Assunção, 2000), control of nonlinear systems, theory of robust filters (Palhares, 1998), and detection, location and quantification of faults (Abdalla et al, 2000; Wang et al, 2007).

### 3.1 Linear Quadratic Regulator using LMIs

Several authors have considered applications of LQR, however, not so many discuss the LMI version of this controller (Johnson et al, 2002). A version of LQR solved by LMIs is presented by Erkus et al (2004). The authors of this contribution show that the problem LQR-LMI is described by:

$$\min_{X, P_{lmi}, X_{lmi}} tr\left([Q_{lqr}][P_{lmi}]\right) + tr\left([X_{lmi}]\right) + tr\left([Y_{lmi}]N\right) + tr\left([N]^T Y_{lmi}{}^T\right) \tag{6}$$

$$\text{subject to} \quad \begin{array}{c} [A][P] - [B][Y_{lmi}] + [P][A]^T - [Y_{lmi}]^T[B]^T + [B_w][B_w]^T < 0 \\ \begin{bmatrix} [X_{lmi}] & [R_{lqr}]^{1/2}[Y_{lmi}] \\ [Y_{lmi}]^T[R_{lqr}]^{1/2} & [P_{lmi}] \end{bmatrix} > 0 \end{array} \tag{7}$$

where $N$ is a noise position vector, $[X_{lmi}]$ and $[Y_{lmi}]$ are the LMIs solutions and tr( ) denote the matrix trace.
The controllers´gain are obtained substituting the matrix $[A]$ by $[[A] - [B_u][KG]]$ in Eq. (7) and solving the Eqs. (6) and (7), where the signal control is $\{u(t)\} = -[KG]\{X(t)\}$ (feedback state control).

### 3.2 Design of robust controllers using LMIs

The major advantage of LMI design is to enable specifications such as stability degree requirements, decay rate, input limitation for the actuators and output peak bounder. It is also possible to assume that the model parameters involve uncertainties (Silva, 2005).
The LMI is a very useful tool for problems with constraints where the parameters vary according to a range of values. The design of robust controllers used in this contribution was presented by Assunção et al (2001). A system with politopic uncertainties is stable if there is $[X]$ e $[G]$ such as the following LMIs are feasible.

$$[A_i][X] - [B_i][G] + [X][A_i]^T - [G]^T[B_i]^T < 0 \tag{8}$$
$$[X] > 0$$

where $i=1,2,…,m$ and $m$ is the number of uncertainties.

Equation (6) was used for the robust control using LQR, and the constraints (Eq. (7)) were arranged in the form given by Eq. (8).

## 4. ELECTROMAGNETIC ACTUATOR (EMA)

The EMA is used to apply the control force to the rotor system. The forces provided by the EMA are inversely proportional to the square of the sum of nominal gap and displacement. With these characteristics, each coil applies a force that is given by Eq. (9).

$$F_{EMA} = \frac{N^2 I^2 \mu_0 af}{2\left((e+\delta)+\dfrac{b+c+d-2a}{\mu_r}\right)^2} \tag{9}$$

The parameters that define the geometry of the coils (*a, b, c, d* e *f*) are shown in the Fig. (2); $\mu_0$ e $\mu_r$ are the magnetic permeability in the vacuum and the relative permeability of the material, respectively. $\mu_r$ is determined experimentally. The gap is given by $e$ and $\delta$ is the gap due to the vibration of the rotor at the position of the electromagnetic actuator.

Four EMAs are used in the system, i.e., two for each control direction (x and z). The EMA applies only attraction force and each actuator acts separately. The ferromagnetic circuit used by each actuator is presented in Fig. (4). The geometry and properties are presented in Tab. (2).
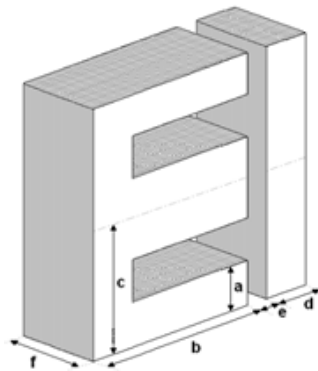


Table 2. Parameters of the coil.

| $\mu_0$ (H/m) | 1.26 X10$^{-06}$ |
|---|---|
| $\mu_r$ | 950 |
| $N$ (spires) | 250 |
| $a$ (mm) | 9.5 |
| $b$ (mm) | 38 |
| $c$ (mm) | 28.5 |
| $d$ (mm) | 9.5 |
| $f$ (mm) | 22.5 |
| $e$ (mm) | 0.5 |

Figure 4. Ferromagnetic circuit.

In the system, there are four actuators. Two in each plan: x plan, actuators 1 and 2, and z plan, actuators 3 and 4. Figure 5 presents the arrangement.
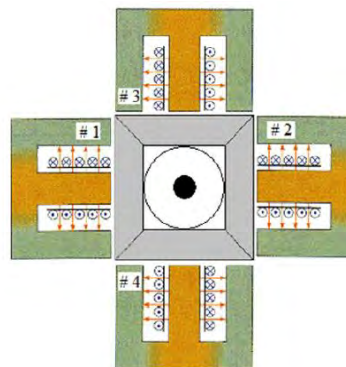


Figure 5. The structure of actuator in the rotor (Morais et al, 2012).

## 5. CONTROL APPROACH

Active modal control is used as control strategy for a rotor system in which an electromagnetic actuator provides the control effort, as shown in the Fig. (6). The advantage of using active modal control is that this technique is very effective for flexible structure applications, requiring a reduced number of actuators and sensors. The estimator is responsible for determining the modal states used in the controllers. The Kalman Estimator is able to estimate the states by using noisy measurement signals.
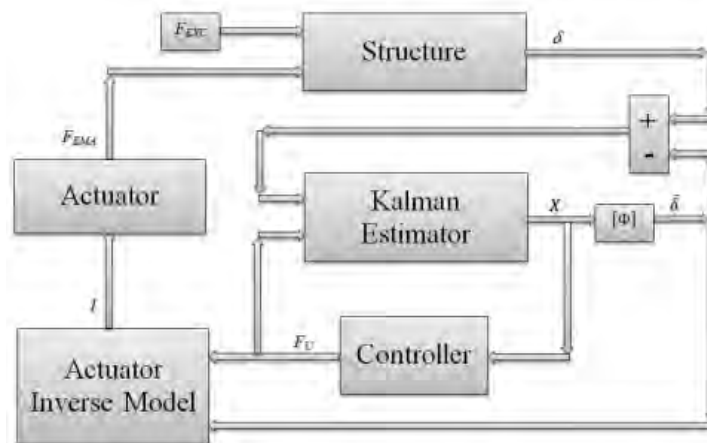
Figure 6. Active modal control based on modal state feedback control.

In this work, robust controllers were developed by using Eqs. (6), (7) and (8).

## 6. RESULTS

Uncertainties were taken into account in the parameters of matrix [*A*], Eq. (3). Regarding the natural frequencies, uncertainties of ±*10*% were considered. To proceed as similar as possible to experimental conditions, band-limited white noise is superimposed to the calculated displacements. Then, the number of modes considered was analyzed in terms of their observability and controllability. For the 4 modes chosen, the system is observable and controllable. The Tab. (3) presents the natural frequencies of the system, with and without uncertainties.

Table 3. Natural frequencies (rad/sec).

| Mode | Without | -10% | +10% |
|---|---|---|---|
| *1* | 160.30 | 143.38 | 175.60 |
| *2* | 160.30 | 143.38 | 175.60 |
| *3* | 623.02 | 557.24 | 682.48 |
| *4* | 623.02 | 557.24 | 682.48 |

With the uncertainties shown in Tab. (3), the uncertain models were obtained. As four uncertainties were considered, 16 uncertain models result. The Tab. (4) presents the 16 uncertain model configurations (matrix $A_i$).

Table 4. Uncertain Model(Matrix $A_i$).

| $A_i$ | Mode 1 | | Mode 2 | | Mode 3 | | Mode 4 | |
|---|---|---|---|---|---|---|---|---|
| | -10% | +10% | -10% | +10% | -10% | +10% | -10% | +10% |
| 1 | X | | X | | X | | X | |
| 2 | X | | X | | X | | | X |
| 3 | X | | X | | | X | X | |
| 4 | X | | X | | | X | | X |
| 5 | X | | | X | X | | X | |
| 6 | X | | | X | X | | | X |
| 7 | X | | | X | | X | X | |
| 8 | X | | | X | | X | | X |
| 9 | | X | X | | X | | X | |
| 10 | | X | X | | X | | | X |
| 11 | | X | X | | | X | X | |
| 12 | | X | X | | | X | | X |
| 13 | | X | | X | X | | X | |
| 14 | | X | | X | X | | | X |
| 15 | | X | | X | | X | X | |
| 16 | | X | | X | | X | | X |

Using these uncertain models, the robust controllers were designed and the following cases were analyzed: impact response and robustness analysis. Only the results in the *x* plane are presented, since the same trends were observed along the *z* plane. The impact was applied in the disk #1 (node #13).
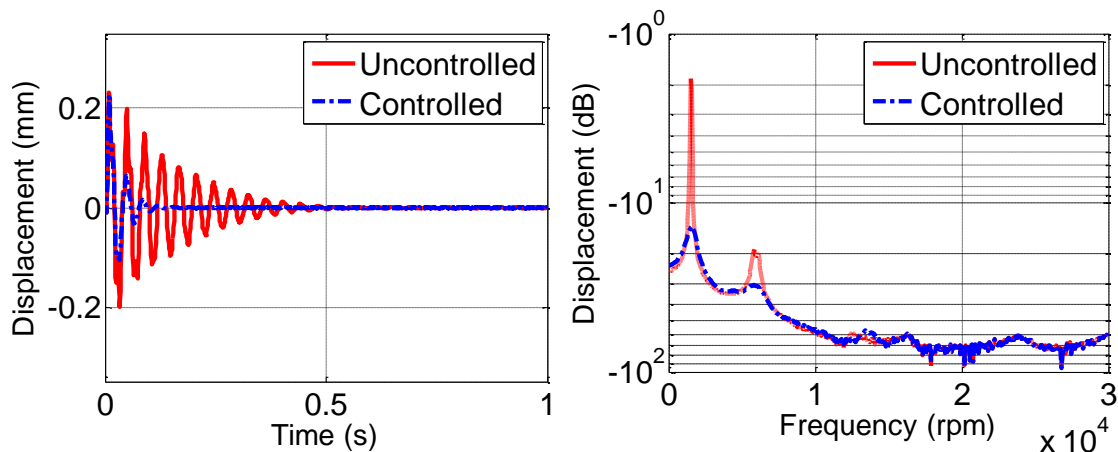
Figure 7. Impact Response and Frequency Response Function (FRF).

The results shown in Fig. (7) demonstrate the effectiveness the proposed control strategy. The amplitude attenuation is obtained for a time smaller than *0.05 sec*. No attenuation was observed for the first overshoot: this occurs because the time response of the estimator has to be taken into account for the reconstruction of the modal states. The same trend was observed for node # 27 and for the *z* direction. The normalized FRFs are presented in Fig. (7). The first two modes in both directions were attenuated (almost *11.18 dB* for the first frequency and *10.65dB* for the second frequency). Besides, no spillover effects are observed for higher modes. The Figs. (8) and (9) present the electrical current required in the *x* plane and the generated electromagnetic force, respectively.
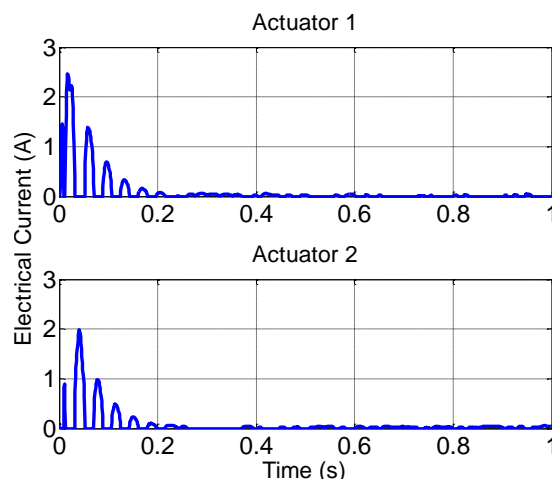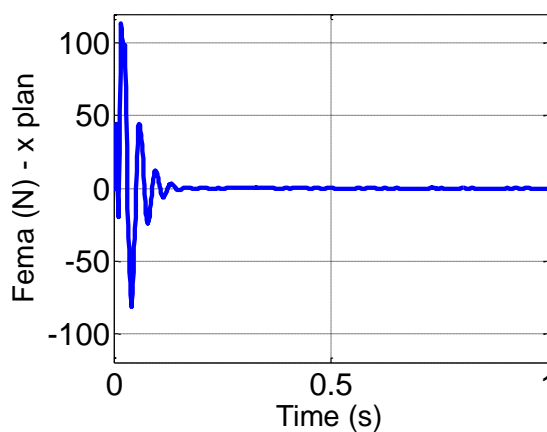


Figure 8. Electrical Current.



Figure 9. Electromagnetic Force.

For analyzing the robustness of the control system, two situations of non-parametric variation are considered in the models. The first consists in applying a variation in the estimator model, and the second consists in analyzing the robust

Koroishi, E. H., Cavalini Jr, A. A., Steffen Jr, V.
Robust Control in Rotor Machines using Linear Matrix Inequalities

controllers for the case in which the uncertain model is considered. The variation of the estimator model corresponds to uncertainties in terms of system identification. The considered variation appears in the dynamic matrix $[A]$ for a variation in the range 0% to +20%. The natural frequencies of the estimator model are presented in Tab. (5).

Table 5. Natural Frequency (Hz) - Estimator.

|  | 0% | +20% |
|---|---|---|
| Mode # 1 | 25.51 | 30.62 |
| Mode # 2 | 25.51 | 30.62 |
| Mode # 3 | 99.16 | 118.99 |
| Mode # 4 | 99.16 | 118.99 |

First, the variation in the estimator is taken into account. The Fig. (10) presents the vibration attenuation for the first and third modes, which correspond the first two modes along the *x* plane.
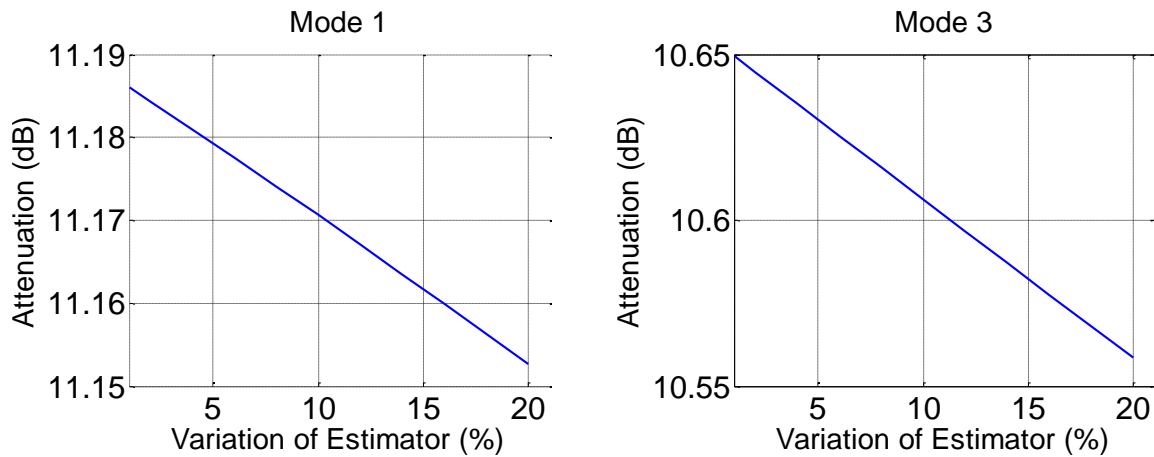


Figure 10. Attenuation for mode #1 and #3.

Figure (10) demonstrates that the controllers are robust with respect to a variation in the model of the estimator. A small variation in terms of attenuation was observed (≈0.03dB for the mode #1 and ≈0.1 dB for the mode #3).

Finally, the robustness was analyzed in terms of uncertain models. The Figs. (11) and (12) present the results for the modes #1 and #3, respectively. The Matrix *A* corresponds to the model without uncertainties, and the matrices $A_i$ (for *i=1,2,...,16*) are the uncertain models shown in Tab. (4).
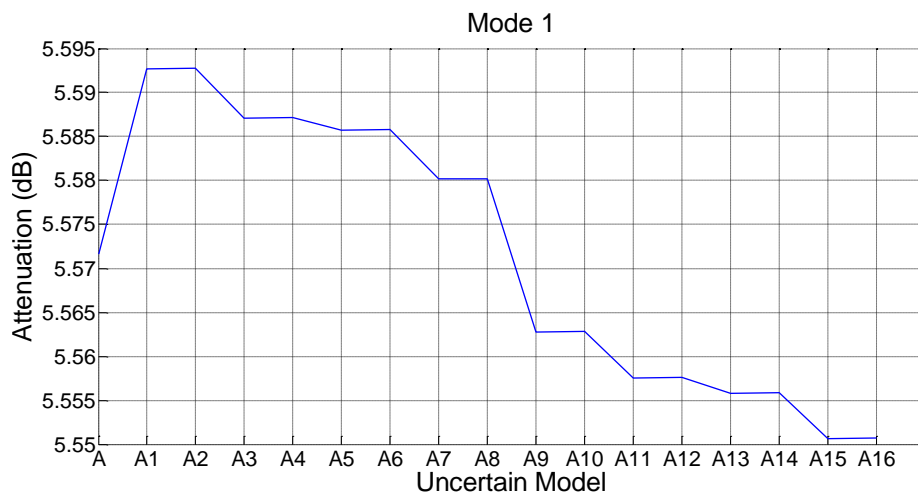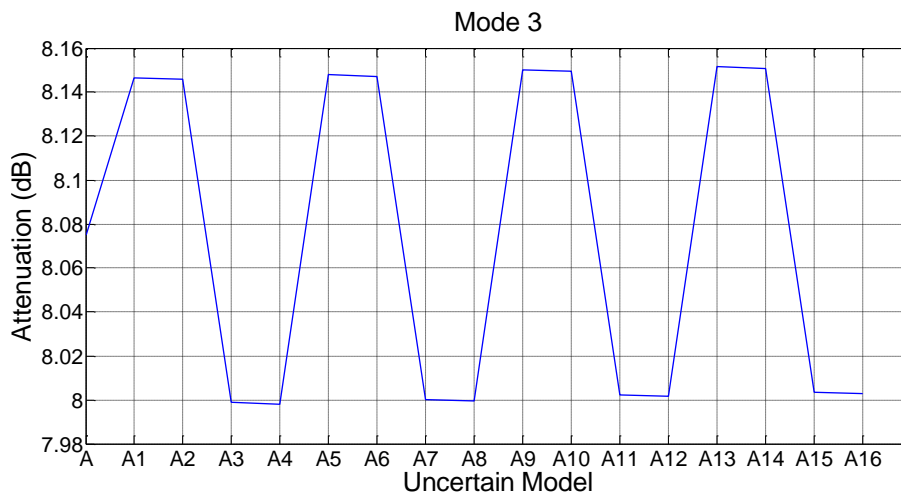


Figure 11. Attenuation for mode #1.

Figure 12. Attenuation for mode #1.

The consideration of uncertain models (see Figs. (11) and (12)) demonstrated the robustness of the controllers. The first mode presents a variation around *0.04*dB, while the second mode presents a variation around *0.15*dB.

## 7. CONCLUSIONS

In this work, a robust control strategy is applied to a rotor system supported by a hybrid bearing formed by a ball bearing and an electromagnetic actuator. The robust controllers were designed by using LQR solved by LMIs. The use of LMIs is an alternative to take into account uncertainties in the model of the system. These uncertainties were introduced considering a non-parametric variation; in this case, the new models ($A_{is}$) correspond to the uncertain models.

For the impact response analysis, the results showed the efficiency of the robust control. This was observed both in the time and frequency domains. In the time domain, the amplitude attenuation was obtained for a time smaller than *0.1 sec*. In the frequency domain, the first two modes were attenuated (about *11.18 dB* for the first frequency and *10.65dB* for the second frequency). It is worth mentioning that no spillover effects were observed in the higher frequencies.

The robustness of the controller was analyzed by considering a variation range from 0 to 20% in the dynamic matrix [*A*] of the estimator and the robustness was also analyzed for each uncertain model ($A_{is}$). The controllers were found to be robust for both cases analyzed. Only small variations were observed in the vibration reduction for each case considered, which demonstrates the effectiveness of the procedure.

Next, the proposed approach will be implemented in a rotor testing machine (see Fig. (2)) in order to validate experimentally the techniques conveyed.

## 8. ACKNOWLEDGEMENTS

## 9. REFERENCES

Abdalla, M.O.; Zimmerman, D.C.; Grigoriadis, K.M., 2000, "Reduce Optimal Parameter Update in Structural Systems Using LMIs", *American Control Conference*, Chicago, Illinois, pp. 991-995.

Assunção, E., 2000, "*Redução H₂ e H∞ de Modelos através de Desigualdades Matriciais Lineares: Otimização Local e Global*" , Tese de Doutorado, UNICAMP, Campinas, SP.

Assunção, E.; Teixeira, M.C.M., 2001, "Projeto de Sistema de Controle Via LMIs usando o MATLAB", *Escola Brasileira de Aplicações em Dinâmica e Controle* – APLICON USP – São Carlos – SP.

Boyd, S., Balakrishnan, V., Feron, E., El Ghaoui, L., 1994, "*Linear Matrix Inequalities in Systems and Control Theory*", Siam Studies in Applied Mathematics, USA, 193p.

Der Hagopian, J., Mahfoud, J., 2010, "Electromagnetic actuator design for the control of light structures", *Smart Structures and Systems*, 6,pp. 29-38.

Erkus, B., Lee, Y. J., 2004, "*Linear Matrix Inequalities and Matlab LMI Toolbox*", University of Southern California Group Meeting Report, Los Angeles, California.

Johnson, E. A. and Erkus, B., 2002, "Structural Control with Dissipative Camping Devices", *American Control Conference*, ACC, Anchorage, Alaska.

Horst, H. G., Wölfel, H. P., 2004, "Active vibration control of a high speed rotor using PZT patches on the shaft surface", *Journal of Intelligent Material Systems and Structures*, 15, pp. 721–728.

Lalanne, M. and Ferraris, G., 1997, "*Rotordynamics prediction in engineering*". John Wiley and Sons, Second Edition.

Morais, T. S., Steffen Jr, V. and Mahfoud, J., 2012, "Control of the breathing mechanism of a cracked rotor by using electro-magnetic actuator: numerical study", *Latin American Journal of Solids and Structures*, 9, pp. 581-596.

Palhares, R. M., 1998, "*Filtragem Robusta: Uma Abordagem por Desigualdades Matriciais Lineares*", Tese de Doutorado, UNICAMP, Campinas, SP.

Palazzolo, A. B., Jogannathan, S., Kascak A. F., Montague, G. T., Kiraly, L. J., 1993, Hybrid active vibration control of rotor bearing systems using piezoelectric actuators, *Journal of Vibration and Acoustics* ,115, pp. 111–119.

Schweitzer, G., Maslen, E. H., 2009, *Magnetic Bearings: Theory, Design and Application to Rotating Machinery*, ISBN 978-3-642-00496-4.

Silva, S., Lopes Jr, V., Assunção, E., 2004, "Robust Control to Parametric Uncertainties in Smart Structures Using Linear Matrix Inequalities", *Journal of the Brazilian Society of Mechanical Science and Engineering*, vol. XXVI, Nº 4, pp. 430-437.

Silva, S., 2005, "*Projeto de Controladores Robustos para Aplicações em Estruturas Inteligentes Utilizando Desigualdades Matriciais Lineares*", Dissertação de Mestrado, Departamento de Engenharia Mecânica, UNESP - Universidade Estadual Paulista, Ilha Solteira, SP, Brasil.

Simões, R. C., Der Hagopian, J., Mahfoud, J., Steffen Jr, V., 2007, Modal active vibration control of a rotor using piezoelectric stack actuators, *J. Vib. Control*, 13, pp. 45-64.

Van Antwerp, J. G., Braatz, R. D., 2000, "A Tutorial on Linear and Bilinear Matrix Inequalities", *Journal of Process Control*, vol. 10, pp. 363–385.

Wang., H. B., Wang, J. L., Lam J., 2007, "Robust Fault Detection Observer Design: Iterative LMI Approaches", *Journal of Dynamic Systems, Measurement, and Control*, vol. 129, ed. 1, pp. 77-82.

## 10. RESPONSIBILITY NOTICE

The authors are the only responsible for the printed material included in this paper.